PIN1-Independent Leaf Initiation in Arabidopsis[1][W][OA]

Bernadette Guenot, Emmanuelle Bayer, Daniel Kierzkowski, Richard S. Smith, Therese Mandel, Petra Žádníková, Eva Benková, and Cris Kuhlemeier*

Institute of Plant Sciences, University of Bern, CH–3013 Bern, Switzerland (B.G., D.K., R.S.S., T.M., C.K.); Laboratory of Membrane Biogenesis, Université Victor Segalen Bordeaux 2, 33076 Bordeaux, France (E.B.); and Department of Plant Systems Biology, University of Ghent, 9052 Ghent, Belgium (P.Ž, E.B.)

Phyllotaxis, the regular arrangement of leaves and flowers around the stem, is a key feature of plant architecture. Current models propose that the spatiotemporal regulation of organ initiation is controlled by a positive feedback loop between the plant hormone auxin and its efflux carrier PIN-FORMED1 (PIN1). Consequently, *pin1* mutants give rise to naked inflorescence stalks with few or no flowers, indicating that PIN1 plays a crucial role in organ initiation. However, *pin1* mutants do produce leaves. In order to understand the regulatory mechanisms controlling leaf initiation in Arabidopsis (*Arabidopsis thaliana*) rosettes, we have characterized the vegetative *pin1* phenotype in detail. We show that although the timing of leaf initiation in vegetative *pin1* mutants is variable and divergence angles clearly deviate from the canonical 137° value, leaves are not positioned at random during early developmental stages. Our data further indicate that other PIN proteins are unlikely to explain the persistence of leaf initiation and positioning during *pin1* vegetative development. Thus, phyllotaxis appears to be more complex than suggested by current mechanistic models.

Phyllotaxis is the regular positioning of lateral organs around a stem (Kuhlemeier, 2007). The divergence angles between successive organs are species dependent but most frequently tend toward 137.5°, which results in spiral phyllotaxis. The 19th century German botanist Wilhelm Hofmeister was the first to meticulously describe a property shared by almost all phyllotactic patterns, now referred to as the Hofmeister rule: new organ primordia are placed in the widest available gap in the meristem, as far away as possible from preexisting primordia (Hofmeister, 1868). This observation, together with primordium isolation experiments (Snow and Snow, 1931; Reinhardt et al., 2005), led to the hypothesis that existing primordia create an inhibition field that suppresses the growth of new organs in their immediate vicinity. A variety of explanations for the nature of inhibition fields has been considered, including mechanisms such as the interplay between tension and compression in the meristem (Green et al., 1996; Shipman and Newell, 2005; Dumais, 2007), contact pressure (Ridley, 1982; Adler et al., 1997), the diffusion of an inhibitory chemical (Schoute, 1913), or the positioning of primordia by underlying vasculature (Larson, 1975). However, molecular and genetic evidence collected in the last decades supports a now widely accepted mechanism of phyllotaxis based on the plant growth hormone auxin and its efflux transporter PIN-FORMED1 (PIN1; Okada et al., 1991; Reinhardt et al., 2003; Jönsson et al., 2006; Smith et al., 2006a). PIN1 is polarized toward regions of high auxin concentrations in shoot apical meristems, thereby reinforcing the accumulation of auxin at convergence points and generating a field of auxin depletion around incipient and bulging primordia (Reinhardt et al., 2003; Heisler et al., 2005; Bayer et al., 2009). Auxin concentrations high enough to trigger PIN1 convergent polarization and subsequent organ induction, therefore, can only appear at a certain distance from preexisting primordia (Reinhardt et al., 2003; Jönsson et al., 2006; Smith et al., 2006a). Hence, the interplay between auxin and its efflux transporter PIN1 provides a plausible molecular mechanism underlying the Hofmeister rule. Such interactions between auxin transport and accumulation are not specific to the shoot meristem. Indeed, the initiation of secondary leaf veins in Arabidopsis (*Arabidopsis thaliana*), the initiation of lateral roots, and the formation of serrations in the leaf margin are based on similar mechanisms of PIN1 polarization toward auxin peaks (Benková et al., 2003; Scarpella et al., 2006; Smith and Bayer, 2009; Bilsborough et al., 2011).

PIN1 is a member of the PIN auxin efflux transporter family with diverse functions in growth and development. A subfamily consisting of PIN5, PIN6, and PIN8 lacks the large hydrophilic loop typically found in other PINs (Paponov et al., 2005). They are not recruited to the plasma membrane but are instead proposed to function as regulators of auxin homeostasis between the cytoplasm and endoplasmic reticulum

[1] This work was supported by the Swiss National Science Foundation; SystemsX.ch, the Swiss Initiative in Systems Biology (to C.K.); and by Starting Independent Research ERC and Central European Institute of Technology grants (to E.B.).

* Corresponding author; e-mail cris.kuhlemeier@ips.unibe.ch.

The author responsible for distribution of materials integral to the findings presented in this article in accordance with the policy described in the Instructions for Authors (www.plantphysiol.org) is: Cris Kuhlemeier (cris.kuhlemeier@ips.unibe.ch).

[W] The online version of this article contains Web-only data.

[OA] Open Access articles can be viewed online without a subscription.

www.plantphysiol.org/cgi/doi/10.1104/pp.112.200402

(Mravec et al., 2009; Wabnik et al., 2011). The other plasma membrane-localized PINs (i.e. PIN1, PIN2, PIN3, PIN4, and PIN7) are involved in processes such as gravitropism, phototropism, embryo development, root meristem regulation, apical hook formation, and shade avoidance responses (Luschnig et al., 1998; Müller et al., 1998; Friml et al., 2002a, 2002b, 2003; Keuskamp et al., 2010; Ding et al., 2011; Rakusová et al., 2011). A complex network of PIN proteins controls patterning and growth in root tips (Blilou et al., 2005; Vieten et al., 2005) and apical hooks (Žádníková et al., 2010). In contrast, only PIN1 has been linked to phyllotaxis and organ initiation in the shoot to date. Indeed, organ initiation is severely impaired in the inflorescence meristem of *pin1* mutants (Okada et al., 1991; Gälweiler et al., 1998), but single mutants of other PINs display no obvious shoot phenotypes under normal growth conditions. Furthermore, the striking pin-shaped inflorescence stalks of *pin1* mutants suggest that other PIN proteins do not rescue organ initiation. Surprisingly, though, *pin1* plants still produce both cotyledons and true leaves during vegetative growth (Okada et al., 1991; Gälweiler et al., 1998), suggesting at least partial rescue of PIN1 loss by other PIN proteins or yet unknown mechanisms during vegetative development. However, little is known about the initiation of rosette leaves in Arabidopsis.

A detailed characterization of the *pin1* vegetative phenotype revealed that the frequency of leaf initiation (plastochron) is irregular and reduced compared with the wild type. However, using a novel quantitative method, we demonstrate that although individual divergence angles are strongly aberrant during early vegetative *pin1* development, leaves are nevertheless positioned nonrandomly, away from existing primordia. We also show that other PIN proteins, which might potentially substitute for PIN1 in the Arabidopsis rosette, are not likely to explain the observed residual leaf positioning mechanism.

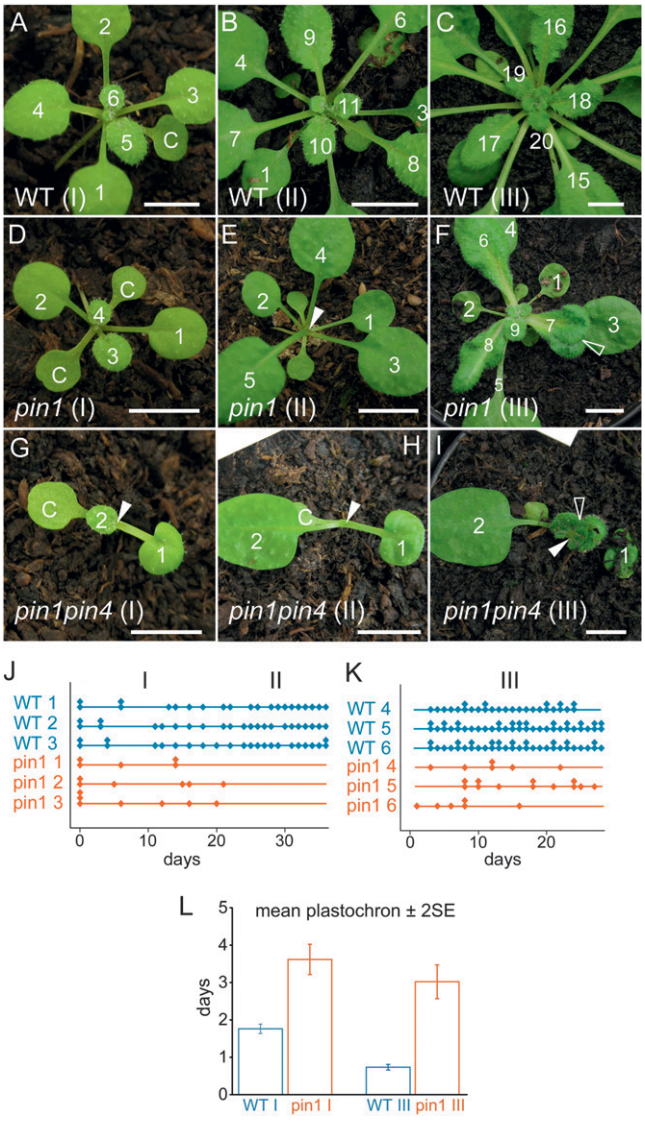

Figure 1. The plastochron is longer and irregular in vegetative *pin1* mutants. A to C, Vegetative development in a wild-type (WT) plant. Leaf initiation and positioning are predictable in wild-type rosettes at stage I (A), stage II (B), and stage III (C). D to F, Vegetative development of a representative *pin1* plant. D, Stage I *pin1* leaves are morphologically similar to the wild type (compare leaf 1 in D with leaf 3 in A and leaf 4 in D with leaf 6 in A). E, Arrest of organ initiation in stage II *pin1*. F, Leaf initiation resumes in stage III, but organs are often fused and misshapen. G to I, Severe vegetative *pin1pin4* phenotype. Severely affected *pin1pin4* mutants often have one cotyledon and produce fewer leaves than *pin1* (G). *pin1pin4* mutants still arrest during stage II (H) and produce fused and misshapen leaves in stage III (I). Closed arrowheads indicate meristems, and open arrowheads highlight fused leaves. Bars = 7 mm. J and K, Graphic representation of organ initiation in stages I and II (J) and stage III (K). Each diamond represents one leaf, and multiple leaves grown on the same day are stacked. The *x* axis represents the number of days since the beginning of observation. Leaves are made regularly in the wild type but not in *pin1*. L, Average plastochrons in the wild type and *pin1*. The mean plastochrons ± 2 SE of wild-type stage I was 1.76 ± 0.06 (n = 555), and the mean plastochron of stage I *pin1* leaves was 3.62 ± 0.20 (n = 181). In stage III, the average plastochron of the wild type was 0.73 ± 0.04 (n = 157) and that of *pin1* was 3.02 ± 0.23 (n = 341).

RESULTS

Three Distinct Stages of Vegetative *pin1* Development

In order to determine to what extent the absence of PIN1 affects leaf initiation in Arabidopsis rosettes, the vegetative phase of *pin1* mutants and wild-type plants was prolonged by growing plants under short-day conditions. In the mutant, three developmental stages with distinct morphological characteristics were observed. Stage I lasted from germination until approximately 3 weeks later. In this early developmental stage, mutants produced morphologically normal leaves whose size, shape, and venation patterns were comparable to those of the wild type (Fig. 1, A and D; Supplemental Fig. S1, A and B). However, the time elapsing between the initiation of two successive leaves, the plastochron, was longer ($P < 0.05$; Fig. 1, J and L) and more variable (Levene's test, $P < 0.01$) compared with the wild type. Although flatter in shape, stage I

mutant meristems had the same layered organization and approximately the same size as wild-type meristems (Fig. 2, A and B).

Stage II took place from 3 to 5 weeks after germination. The initiation of organs was completely abolished for the duration of this intermediate stage (Fig. 1, B, E, and J). However, histological sections showed a normally organized meristem during stage II (Fig. 2, C and D). Toward the end of stage II, an area of small cells ("zone of no distinction") was observed around the meristem, indicating that the arrest of leaf initiation was not accompanied by an arrest of meristematic cell proliferation (Fig. 2, D, G, and L).

Stage III started approximately 5 weeks after germination and ended with the transition to flowering (Fig. 1, C and F). Although organ initiation resumed during this stage, the leaves produced clearly differed from the ones initiated during stage I. Stage III leaves were often fused and epinastic, tended to form several lobes on the same leaf blade, and had particularly broad petioles (Fig. 1F, open arrowhead). Furthermore, venation in these leaves was clearly aberrant, and the fusion of multiple veins into a pseudo-midvein resembled venation patterns obtained after treatment with the auxin efflux inhibitor *N*-(1-naphthyl) phthalamic acid (Supplemental Fig. S1; Mattsson et al., 1999; Sieburth, 1999). Histological sections, together with the unaltered expression of the central zone marker CLAVATA3-GFP in *pin1*, indicated that the meristem remained organized and active at stage III (Fig. 2, E, F, H, and I) and after bolting (Fig. 2, J and K). The plastochron in stage III mutants was longer than in the wild type ($P < 0.05$; Fig. 1, K and L) and had a higher SD (Levene's test, $P < 0.01$) due to the simultaneous initiation of multiple leaves on the one hand and the occasional temporary arrests of organ initiation on the other hand.

Leaf Positioning Is Not Random in *pin1* Stage I Plants

In addition to leaf initiation frequencies, we also characterized leaf positioning in *pin1* mutants. The divergence angles of leaves initiated during stage I strongly deviated from the average 137° angle found in wild-type plants (Fig. 3, A and B). However, divergence angles at stage I seemed to be not entirely random (e.g. clusters of overlapping leaves were not observed; Fig. 3C). From the graph of the divergence angles (Fig. 3B), it is unclear if an organ-spacing mechanism is still controlling organ position. In order to quantify to what extent leaves continued to select their position "as far as possible from previous leaves," we devised a new index, which we named the Hofmeister index (HI). It is based on Hofmeister's idea that new leaf primordia tend to form as far as possible from preexisting ones. This simple spacing mechanism implemented on a growing shoot apex has been shown to be capable of reproducing all of the common phyllotaxis patterns observed in nature (Douady and Couder, 1996; Smith et al., 2006b). In these models, leaf primordia produce an inhibitory field suppressing organ formation nearby, without specifying the molecular mechanism. New organs appear at the area of lowest inhibition when the inhibition drops below a threshold level. Following Smith et al. (2006b), we suppose that the inhibitory field decreases with a primordium's age and distance from the peripheral zone. To define the HI, we calculate inhibition fields around organs placed as observed in our time-lapse data. We define the HI as the difference between the calculated position of lowest inhibition (Fig. 3E, orange dot) and the actual position of organ outgrowth (Fig. 3E, red dot). Thus, the measure is not just a simple angular displacement from the previous leaf but takes into account the influence of older leaves as well (Fig. 3E). Note that such a measure is independent of the particular phyllotaxis type and works equally well for patterns with different divergence angles, during transitions, and with decussate and multijugate patterns. Leaves with a small HI have grown in a region of the meristem where little inhibition from previous primordia is expected. The minimum possible HI is 0 if a primordium grows at the position of minimal inhibition and approximately 1 for primordia growing on top of each other.

Series of divergence angles and leaf ages were derived from time-lapse imaging of stage I wild-type and *pin1* plants. Interestingly, no correlation was found between plastochron length and divergence angles (Supplemental Fig. S2). For every observed leaf, an inhibition profile was calculated based on the relative position and age of previous leaves. There was no significant difference between the average HI of the wild type and *pin1* ($P > 0.05$), which scored 0.010 and 0.009, respectively (Fig. 3D). However, both wild-type and *pin1* leaves had smaller and less variable HI values than the random control of simulated plants with randomly generated leaves, which had an average HI of 0.159 ($P < 0.01$). It was not possible to adequately measure divergence angles to use with the HI model on stage III *pin1* mutants. Stage III primordia tended to fuse during postmeristematic development, making it impossible to deduce angles and ages that correctly reflect the situation in the meristem from image series. However, we observed that approximately one-half (18 of 31) of dissected stage III meristems had clusters of organs that violated Hofmeister's rule (Fig. 2L).

To summarize, we found that although the timing of organ initiation was affected in *pin1* mutants and the individual divergence angles were clearly aberrant, the positioning of leaves in stage I mutants was nonrandom and largely obeyed Hofmeister's rule. During stage II, leaf initiation ceased and small cells (zone of no distinction) formed at the flanks of the meristem. At stage III, leaf initiation resumed but positioning was aberrant. In addition, organs produced late in *pin1* development were frequently fused and had aberrant shapes and venation patterns.

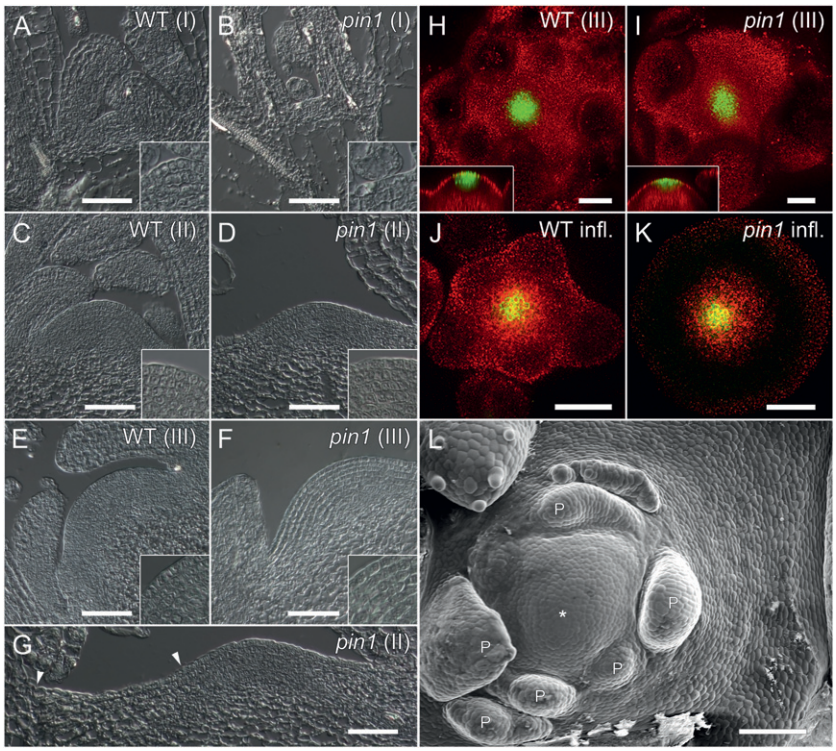

Figure 2. Meristem organization in wild-type (WT) and *pin1* Arabidopsis. A and B, Longitudinal sections through stage I meristems (10 d after germination). *pin1* meristems (B) are comparable to the wild type (A) in size and structure but tend to be flatter. C and D, Stage II meristems (4 weeks old). Both wild-type (C) and *pin1* (D) meristems are organized in layers and structurally intact. E and F, Stage III meristems (6 weeks old). Wild-type (E) and *pin1* (F) meristems are of similar size and structure. G, Zoom out of D. Even though organs are not initiated in stage II *pin1* mutants, meristem growth is not arrested, as evidenced by the small cells (zone of no distinction) between stage I leaves and the meristem boundary (arrowheads). Insets are closeups of the central meristem regions. H to K, Expression of the central zone marker CLV3-GFP is comparable in stage III meristems of the wild type (H) and *pin1* (I) as well as in inflorescence wild-type (J) and *pin1* (K) meristems. L, Scanning electron microscopy image of a stage III *pin1* meristem. Primordia (P) are poorly spaced and clustered on one side of the meristem. The zone of no distinction produced during stage II is clearly visible. The asterisk shows the center of the meristem. Bars = 50 μm in A to K and 100 μm in L.

DR5 Expression Is Initially Normal But Becomes Increasingly Aberrant during Later Stages of *pin1* Development

Since the stage-dependent differences in leaf initiation and positioning are likely linked to differences in auxin dynamics, we analyzed auxin distributions in *pin1* mutants of all stages using the synthetic auxin response reporter DR5-GFP (Benková et al., 2003). Stage I wild-type seedlings showed DR5-GFP expression in leaf tips, early veins, and stipules (Fig. 4A). Approximately 60% (10 of 17) of wild-type seedlings displayed DR5-GFP expression in the shoot apical meristem (Fig. 4A). The absence of DR5 signal in part of the wild-type seedlings is most likely due to the long plastochron, because leaf primordia are not being initiated at the time of observation. We analyzed a large population of seedlings segregating for the *pin1* allele, assuming that any change in DR5-GFP due to the loss of PIN1 should be visible in one-fourth of them. All analyzed seedlings showed similar DR5-GFP expression as wild-type seedlings (Fig. 4B). As in wild-type seedlings, 64% (27 of 42) of the seedlings segregating for the *pin1* mutation had DR5-GFP signal in the meristem itself (Fig. 4B). Therefore, we conclude that within the resolution of the experiment, the DR5 expression patterns were similar between the *pin1* mutant and the wild type.

In wild-type plants, during stages II and III and after bolting, DR5-GFP was expressed in regularly spaced peaks in young and incipient primordia (Fig. 4, C, E, and G). In contrast, DR5-GFP expression in *pin1* clearly differed from the wild type in stage II and III mutants. Stage II meristems were often surrounded by very strong DR5-GFP signal (10 of 12), but DR5-GFP was usually not detectable in the meristem itself (10 of 12; Fig. 4D). During stage III, DR5-GFP levels were again very high in the tissue subjacent to the meristem (41 of 41; Fig. 4F). However, it was difficult to draw conclusions about leaf development in stage III plants because DR5-GFP was never visible in young primordia of mutant stage III meristems, suggesting that the DR5 promoter might not be responsive in those tissues. Signal intensities in the meristem itself varied from very high (Fig. 4F, inset; eight of 41) or comparable to the wild type (Fig. 4F; 22 of 41) to very low or undetectable (Fig. 4F, inset; 11 of 41). In mutants with DR5-GFP expression within the meristem, no obvious signal maxima were observed. After bolting, DR5-GFP was only found at very low levels in a few dispersed cells of mutant inflorescence meristems (Fig. 4H). In conclusion, no difference of DR5-GFP expression was detected in stage I wild-type and *pin1* mutant plants. The organ arrests in *pin1* stage II and inflorescences correlated with a lack of DR5-GFP in the meristem, while the organ initiation activity of stage III meristems was consistent with variable levels of DR5-GFP expression.

Only PIN1-GFP Is Expressed in the Meristem

We hypothesized that leaf initiation and spacing in *pin1* might be regulated by the activity of other PIN proteins in the vegetative meristem. Therefore, we analyzed the expression patterns of the other plasma

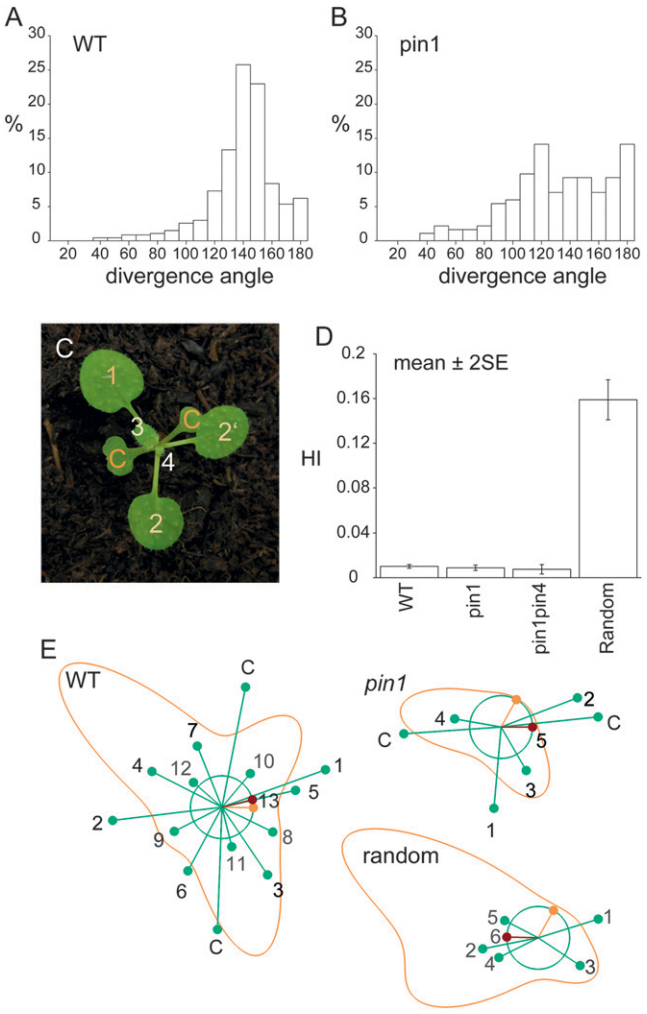

Figure 3. Divergence angles in *pin1* and *pin1pin4* mutants are aberrant but spacing is nonrandom. A, Divergence angles in the wild type (WT). The distribution has a clear peak around the ideal angle of 137.5°. B, Divergence angles in *pin1*. The angles vary widely. C, Leaf positioning in *pin1*. Despite the deviation from typical wild-type angles, leaves are placed according to the Hofmeister rule (compare the positioning of leaf 1 with regard to the cotyledons and the position of leaf 2 with regard to the previously initiated leaves). D, Average HI ± SE. The HI values for the wild type (0.010; $n = 544$), *pin1* (0.009; $n = 229$), and *pin1pin4* (0.007; $n = 144$) were not significantly different among themselves ($P > 0.05$) but were clearly smaller than the HI of the random control (0.159). The SD in the random control was clearly higher than in measured plants (Levene's test, $P < 0.01$). E, Visualization of the HI simulation. Green circle, ring of organ initiation; green dots, older primordia; red dot, actual position of the newest primordium; orange dot, ideal position for the newest primordium (minimum inhibition); orange line, inhibition profile. Primordia are labeled in order of appearance. C, Cotyledon.

membrane-associated PIN efflux carriers PIN2, PIN3, PIN4, and PIN7 in wild-type and *pin1* vegetative meristems using translational GFP fusions under the control of their native promoters.

In stage I wild-type seedlings, PIN1-GFP was expressed in the epidermis and vasculature of leaf primordia as well as in the meristem itself (Fig. 5A). None of the other PIN-GFP constructs was detected in the meristem (Fig. 5, B–E). PIN2-GFP was expressed in a single row of leaf margin cells with polarization toward leaf tips (Fig. 5B). PIN3-GFP was found in the epidermis of leaf primordia and cotyledons (Fig. 5C). While it was difficult to determine the polarization of PIN3-GFP in cotyledons and older leaves, it was pointing up in the epidermis of

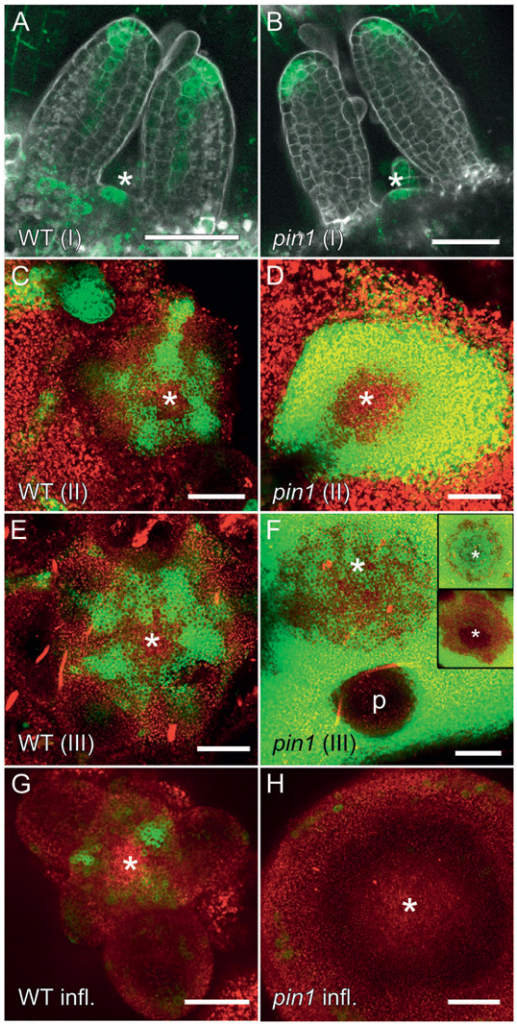

Figure 4. DR5-GFP expression in vegetative and inflorescence stage *pin1* apices. A and B, Vegetative stage I (5 d after germination). DR5-GFP expression does not significantly differ from the wild type (WT; A) in *pin1* seedlings (B). C and D, Vegetative stage II (4 weeks after germination). While wild-type plants have clearly visible DR5-GFP peaks (C), *pin1* mutants show strong DR5-GFP signal surrounding the meristem (D). E and F, Vegetative stage III (6 weeks after germination) wild-type (E) and *pin1* (F) meristems. In *pin1*, DR5-GFP is highly expressed in differentiated "stem" tissues outside of the meristem, but signal intensity is variable in meristems. Insets show extremes of DR5-GFP expression in *pin1* (F). p, Primordium. G and H, Inflorescence stage. Consistent with previous publications, DR5-GFP is expressed in peaks at incipient and young primordia (G) but is detectable in only a few, scattered cells in *pin1* inflorescence apices (H). Asterisks indicate meristem positions. Bars = 50 μm.

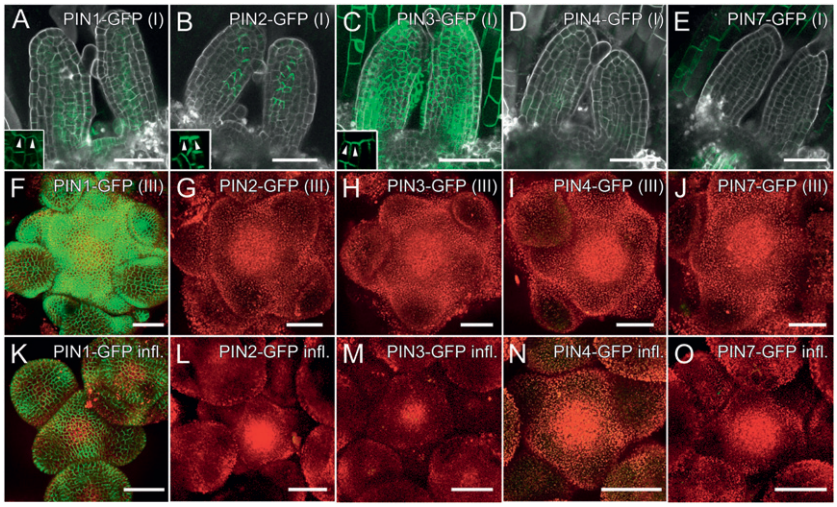

Figure 5. Only PIN1 is expressed in wild-type Arabidopsis meristems. A to E, Expression of PIN-GFP fusions in vegetative stage I (5 d after germination). A, PIN1-GFP is expressed in the meristem and vasculature of seedlings as well as in part of the epidermis. The inset shows upward polarization of PIN1-GFP in the epidermis (arrowheads). B, PIN2-GFP is polarized upward in leaf margin cells. The inset shows PIN2-GFP polarization (arrowheads). C, PIN3-GFP is present in the epidermis of young primordia and cotyledons. The polarization of PIN3-GFP is initially upward (inset; arrowheads) but later becomes indistinguishable in mature tissues. D, PIN4-GFP is expressed very weakly in seedling epidermis. E, PIN7-GFP is not found in meristems or young primordia but in the epidermis of cotyledons and older leaves (data not shown). F to J, Vegetative stage III (6 weeks after germination). F, PIN1-GFP is expressed throughout the epidermis of meristems and primordia. G to J, PIN2-GFP (G), PIN3-GFP (H), PIN4-GFP (I), and PIN7-GFP (J) were not detected in stage III meristems. K to O, Inflorescence stage. PIN1-GFP was visible in the epidermis of meristems and primordia (K), but expression of PIN2-GFP (L), PIN3-GFP (M), PIN4-GFP (N), and PIN7-GFP (O) was not detected. Bars = 50 μm.

primordia (Fig. 5C, inset). The polarization of PIN1-GFP, PIN2-GFP, and PIN3-GFP toward the leaf tip in the epidermis of primordia is consistent with a postulated flux of auxin from the meristem toward the tip of initiating organs (Benková et al., 2003; Reinhardt et al., 2003). PIN4-GFP was occasionally expressed very weakly in the epidermis of primordia (Fig. 5D). PIN7-GFP was found in a pattern very similar to PIN3-GFP in hypocotyls as well as in the epidermis of young leaves but was not found in young primordia (Fig. 5E). In stage III and inflorescence meristems, PIN1-GFP was the only PIN protein found in the meristem or young primordia (Fig. 5, F–O).

Ectopic up-regulation of PIN proteins in *pin* mutant combinations has been reported in roots (Blilou et al., 2005; Vieten et al., 2005). Therefore, we hypothesized that PIN proteins might likewise be up-regulated in the shoot meristem in the absence of PIN1. To address this question, we crossed all four GFP constructs into the *pin1* background. In segregating populations of stage I seedlings, all analyzed PIN2-GFP*pin1* (n = 63), PIN4-GFP*pin1* (n = 73), and PIN7-GFP*pin1* (n = 69) meristems showed expression patterns comparable to wild-type populations (Supplemental Fig. S3, A, C, and D). No up-regulation of other PINs was found in stage III or inflorescence meristems, either (Supplemental Fig. S3). In the case of PIN3-GFP, most lines resulting from the cross of PIN3-GFP into the *pin1* background showed expression similar to the wild-type background (Supplemental Fig. S3, B and F). However, some lines expressed PIN3-GFP in bulging primordia of stage I and stage III plants (Supplemental Fig. S3, M and N). This ectopic expression was not specifically due to the *pin1* mutation, because it was also observed in phenotypically wild-type plants of those crosses (Supplemental Fig. S3, P and Q). However, *pin1* mutants with such ectopic PIN3-GFP expression were phenotypically undistinguishable from *pin1*. In other words, this ectopic PIN3 expression did not rescue the lack of PIN1 function. In summary, PIN2-GFP, PIN3-GFP, and PIN7-GFP were expressed at different stages of primordium development, but only PIN1-GFP was found in the meristem or in incipient primordia at any stage of wild-type development. Occasional ectopic expression of PIN3-GFP had no effect on the *pin1* phenotype. Furthermore, none of the analyzed PIN proteins was up-regulated in meristems in the *pin1* background.

Additional *pin* Mutations Do Not Exacerbate Early Leaf Positioning

Although none of the other PINs was found in the meristem itself, they might still influence phyllotactic patterning from a distance, for instance by turning existing primordia into auxin sinks. To test this hypothesis, we crossed the *pin2*, *pin3*, *pin4*, and *pin7* mutants, which have no obvious phyllotactic phenotype

under normal growth conditions, into the *pin1* background. No double mutant combination showed an increased phenotypic severity compared with *pin1*, except for *pin1pin4*. A high proportion of *pin1pin4* seedlings had a single cotyledon (60.1%, $n = 198$, compared with 3.9% in *pin1*, $n = 153$; Supplemental Fig. S4A). Furthermore, the average plastochron of *pin1pin4* leaves (5 d; $n = 154$) was significantly longer than in *pin1* ($P < 0.05$). Stage I *pin1pin4* mutants were smaller, their average leaf surface reaching only 40% of *pin1* area (*pin1*, $n = 30$; *pin1pin4*, $n = 36$). However, despite this more severe shoot phenotype, leaves were still placed according to Hofmeister's rule in stage I *pin1pin4* mutants, with an average HI of 0.007, which was not significantly different from *pin1* ($P < 0.05$; Supplemental Fig. S4B). As a result, in seedlings with only one cotyledon, the first, and sometimes also the second true leaf were positioned at an angle of 180° (eight of 31; Fig. 1, G and H). Since PIN4-GFP is virtually absent in the shoot apex, we favor the hypothesis that the distichous arrangement of the first few leaves in monocotyledonous *pin1pin4* mutants is a consequence of its embryonic defects. Therefore, our analysis of double mutants indicates that none of the four other plasma membrane-localized PINs is essential for leaf formation and positioning in vegetative *pin1* mutants.

DISCUSSION

The positive feedback loop between auxin and its transporter PIN1 is thought to regulate both leaf positioning and leaf initiation. PIN1 and DR5 are strongly expressed at the location of future organ development (Reinhardt et al., 2003; Heisler et al., 2005; Bayer et al., 2009), and the inhibition of PIN1 activity in Arabidopsis either by genetic means or through the use of the auxin polar transport inhibitor *N*-(1-naphthyl) phthalamic acid results in the formation of naked, pin-shaped inflorescences (Okada et al., 1991). However, the *pin1* phenotype is far less drastic at the cotyledon and vegetative phases compared with inflorescence meristems, in which the formation of lateral organs is almost completely lost (Figs. 1 and 2; Supplemental Fig. S4, C and D). In the Arabidopsis relative *Cardamine hirsuta*, inactivation of the PIN1 ortholog causes a similar phenotype, with a severe reduction of organ formation in the inflorescence but much milder effects in the vegetative phase (Barkoulas et al., 2008). Inhibition of auxin transport with chemical inhibitors indicates strong effects in young tomato (*Solanum lycopersicum*) and maize (*Zea mays*) seedlings (Reinhardt et al., 2000; Scanlon, 2003). However, *pin* knockout mutants will be needed to clarify the role of individual transporters in phyllotactic patterning in other angiosperm families.

Our detailed characterization of the vegetative *pin1* phenotype shows that the plastochron is longer and more variable in mutants than in the wild type. However, although the divergence angles between successive leaves are aberrant and do not conform to the typical 137° angles found in the wild type, organs are still initiated according to the Hofmeister rule in early stages of *pin1* vegetative development. We demonstrated this using a novel index, which takes into account the age and positioning of all the leaves produced throughout a plant's lifetime. Such a method is necessary because traditional angle histograms only consider angles between two successive leaves, which obscures potential nonrandomness when both angles and plastochron are variable. An approach frequently used in the study of phyllotaxis is the calculation of Shannon entropies as a measure of randomness, which is useful for the study of switches between regular phyllotactic patterns but less so for the quantification of early *pin1* mutants (Itoh et al., 2000; Barabé and Jeune, 2006; Prasad et al., 2011). In contrast, the HI takes into account the entire developmental history of a plant and therefore is well suited to detect variable, but nonrandom, patterns. To summarize, the HI reveals that in the absence of PIN1 or other PIN proteins, leaves are positioned away from the inhibiting effect of existing primordia. Thus, organ positioning, although not perfect, can proceed even in the absence of PIN1.

The severity of the vegetative *pin1* phenotype increases with time, until organ initiation finally arrests upon floral induction. This stage-dependent phenotypic severity is mirrored by anatomical and molecular features. An obvious explanation for the phenotypic differences between early and late *pin1* development would be that other PIN proteins substitute for the loss of PIN1 only in early vegetative phases. Therefore, we set out to determine which of the other plasma-localized PIN proteins could compensate for the loss of PIN1 in the rosette. Surprisingly, we found that PIN2-GFP, PIN4-GFP, and PIN7-GFP are not expressed in the meristem. The PIN3-GFP construct is strongly expressed in the vicinity of the meristem, and a few PIN3-GFP lines displayed some meristematic expression (Fig. 5; Supplemental Fig. S3). However, all PIN3-GFP/*pin1* lines were phenotypically indistinguishable from *pin1*, indicating that PIN3 expression does not complement the lack of PIN1. Therefore, we hypothesized that leaf initiation and positioning in *pin1* may be complemented by the activity of transporters expressed outside the meristem. An attractive scenario could be that polar localization of PINs within a young primordium drains auxin from the meristem and thereby creates local auxin maxima away from the young primordium, leading to a residual leaf-positioning mechanism. Double mutants of *pin2*, *pin3*, and *pin7* with *pin1* are indistinguishable from *pin1*. Although the *pin1pin4* mutant has a more severe phenotype, we prefer the conservative interpretation that this is the consequence of defects in the embryo.

Our conclusion that other PINs do not substitute for PIN1 is based on two different approaches: analysis of mutants in all the plasma membrane-localized PINs and PIN-GFP expression data. Although other scenarios perhaps cannot be categorically excluded, we believe that the combination of approaches makes this

conclusion convincing. The question thus arises how meristems form nonrandomly distributed leaves in the absence of PIN activity. Possibilities are other auxin transporters, auxin synthesis, and auxin-independent mechanisms of leaf initiation in Arabidopsis. Other auxin transporters that might be functional in the meristem include the AUX1/LAX auxin importers, the ATP-binding cassette (ABC) auxin efflux transporters, and as yet uncharacterized auxin transporters. The *aux1lax1lax2lax3* quadruple auxin importer mutant has temporary arrests of leaf initiation under short days and is almost normal under long days (Bainbridge et al., 2008). When the *pin1* mutant is combined with mutants in AUX1 and LAX1, the two proteins that are coexpressed with PIN1 in the L1 surface layer, the triple mutant continues to make leaves (Supplemental Fig. S5). Therefore, it seems unlikely that auxin influx carriers play a crucial role in vegetative organ initiation. The ABC family of auxin efflux transporters are thought to be apolarly localized in the shoot and responsible for long-range transport of auxin in the vasculature rather than for phyllotactic patterning (Geisler et al., 2005; Mravec et al., 2008; Verrier et al., 2008; Lewis et al., 2009). However, only a few members of the large ABC family have been analyzed to date, and currently it cannot be excluded that one of the 21 related Arabidopsis ABCs could play a role in phyllotaxis (Jasinski et al., 2003; Geisler et al., 2005; Mravec et al., 2008). It also cannot be excluded that other, as yet unknown, auxin transporters might influence organ initiation.

A second possibility is that local auxin synthesis in the vegetative meristem might lead to leaf initiation. Whether auxin is synthesized within the meristem or needs to be imported from outside is the subject of much debate. It has been suggested that auxin is imported from source organs, such as mature leaves, into the meristem via epidermal PIN1 (Ljung et al., 2001; Reinhardt et al., 2003). This hypothesis is consistent with the massive accumulation of the DR5-GFP auxin reporter at the border of vegetative *pin1* meristems as well as the auxin depletion found in inflorescence meristems (Fig. 4; for a discussion of the limitations of the DR5 reporter, see Vernoux et al., 2011). It is possible that active auxin transport is absolutely required in the rapidly extending inflorescence stem but that vegetative meristems acquire sufficient auxin through diffusion to allow leaf initiation, albeit more slowly and less regularly. On the other hand, there is also evidence for the expression of key biosynthetic genes in the meristem (Cheng et al., 2006, 2007; Mashiguchi et al., 2011; Stepanova et al., 2011; Won et al., 2011; Yoshida et al., 2011). While the biosynthetic *yuc1yuc4* double mutant makes leaves, introducing *yuc1yuc4* into the *pin1* background completely suppresses postembryonic leaf formation (Cheng et al., 2007). This suggests that local auxin production in the meristem enables the initiation of leaves in *pin1*, but it is not sufficient to provide the constant auxin supply necessary for correct wild-type phyllotactic patterning without auxin efflux carriers. Hence, PIN1 may have the additional and unique function of maintaining auxin homeostasis in the meristem.

A third possibility is that a nonauxin mechanism may support phyllotactic patterning and organogenesis in vegetative meristems. Attention has shifted in recent years from the classical notion of a primordium-based inhibitory signal toward PIN-based models, in which auxin is an inductive signal that is redistributed within the meristem. Nevertheless, an inhibitor that diffuses from the primordia and inhibits organogenesis in the vicinity of a previously initiated primordium remains a plausible option. For instance, a hypothetical primordium-derived signal might diffuse into the meristem and activate *KNOX* gene expression, which acts to antagonize organogenesis nearby. Light through cytokinin affects phyllotaxis, and interactions between auxin and cytokinin have been demonstrated within the meristem (Zhao et al., 2010; Yoshida et al., 2011). It is possible, therefore, that cytokinin stabilizes phyllotaxis, probably indirectly through its effect on meristem size. Furthermore, the concept of phyllotactic patterning through tissue mechanics also has a long history and recently gained experimental support (for review, see Braybrook and Kuhlemeier, 2010; Besnard et al., 2011). The local application of cell wall-modifying proteins such as expansins and pectin methylesterases induces local organ outgrowth, followed by a modification of subsequent phyllotaxis (Fleming et al., 1997; Pien et al., 2001; Peaucelle et al., 2008). This suggests that changing mechanical properties of the cell wall can influence organ positioning. It is conceivable that such a physical mechanism would suffice to maintain residual phyllotactic patterning in the absence of auxin/PIN-based mechanisms.

MATERIALS AND METHODS

Plant Material and Growth Conditions

Arabidopsis (*Arabidopsis thaliana*) CLV3-GFP (Lenhard and Laux, 2003), ProPIN1:PIN1-GFP (Benková et al., 2003), ProPIN2:PIN2-GFP (Xu and Scheres, 2005), ProPIN3:PIN3-GFP (Žádníková et al., 2010), ProPIN7:PIN7-GFP (Blilou et al., 2005), and DR5-GFP (Benková et al., 2003) have been described previously. The ProPIN4:PIN4-GFP construct was described by Vieten et al. (2005). The functionality of the PIN-GFP constructs was tested in roots before use (data not shown). The *pin1-7* (Smith et al., 2006a) allele was used for all crosses involving *pin1*. *eir1-1* (N8058), *pin3-5* (N9364), *pin4-3* (N9368), and *pin7-2* (N9366) were obtained from the Nottingham Arabidopsis Stock Center. All mutant alleles are in the Columbia background. Root gravitropism assays were used to screen for homozygous *pin2* plants and lines during crosses. All other mutant alleles were genotyped using PCR (*pin1-7*, 5′-TTCCATAAAGTCATGATTAAGCACA-3′, 5′-CGGTGGGAACAACATAAGCAA-3′, and 5′-GCGTGGACCGCTTGCTGCAACT-3′; *pin3-5*, 5′-CCCATCCCCAAAAGTAGAGTG-3′, 5′-GGAAGTGTGGAGAGGGAAAAG-3′, and 5′-ATTTTGCCGATTTCGGAAC-3′; *pin4-3*, 5′-CAACGCCGTTAAATATGG-3′, 5′-TTCCCACTACAATTATTCC-3′, and 5′-TGCAGCAAAACCCACACTTTTACTTC-3′; *pin7-2*, 5′-TTTACTTGAACAATGGCCACAC-3′, 5′-GGTAAAGGAAGTGCCTAACGG-3′, and 5′-ATTTTGCCGATTTCGGAAC-3′). For each of these three-primer PCR assays, the first two listed are gene-specific forward and reverse primers and the third primer anneals inside the mutagenic transposon. Mutant alleles produce shorter (approximately 700 bp) bands, while wild-type allele products are longer (around 900–1,000 bp). For the analysis of inflorescence meristems, plants were grown under long-day

conditions (16 h of light, 60% humidity, 20°C day temperature, irradiance of 110 μE m^{-2} s^{-1}). For all other experiments, plants were grown under short-day conditions (8 h of light, 60% humidity, 20°C–22°C day temperature, irradiance of 150 μE m^{-2} s^{-1}).

Microscopy and Imaging

For scanning electron microscopy, samples were dissected, immediately frozen at −20°C, and imaged using a Hitachi S-3500N variable-pressure scanning electron microscope. For the observation of venation patterns, leaves were cleared in 70% ethanol at 37°C overnight. For histological sections, plant materials were fixed and sectioned as described by Reinhardt et al. (2003).

Fluorescent signals were detected using 20% of the possible power supply of the 488-nm argon laser on a Leica upright confocal laser-scanning microscope (Leica TCS SP5). The emission bandwidth was set to 500 to 550 nm for GFP, 620 to 700 nm for autofluorescence, and 625 to 680 nm for propidium iodide. Laser strength was modulated by setting the acousto-optic tunable filter values to 30% (for DR5-GFP in stage II, stage III, and inflorescence), 40% (stage I DR5-GFP and PIN-GFP), or 80% (stage III and inflorescence PIN-GFP). Stage II, stage III, and inflorescence meristems were visualized immediately after dissection to avoid stress-induced wound responses using a long-working-distance water-immersion 20× lens. Stage I seedlings were incubated in 0.1% propidium iodide solution for 10 min, rinsed in distilled water, dissected, transferred to glass slides, and observed using a close-working-distance 20× magnification lens. Stage II, stage III, and inflorescence meristems are shown as overlays of maximum intensity projections from the GFP and autofluorescence channels. For stage I meristems, maximum intensity projections of GFP channels were overlaid with single optical sections of propidium iodide using the linear dodge (add) layer mode in Adobe Photoshop. Propidium iodide and autofluorescence images were adjusted using a curve adjustment layer in Photoshop when necessary.

Angle Measurements and HI

For developmental time series, photographs of plants were taken from above every 2 d using a Canon IXUS 80 IS compact digital camera. Divergence angles were measured using MacBiophotonics ImageJ.

The HI was calculated using a C++ program written in L-studio (Prusinkiewicz, 2004) and VVe modeling environments. Using the single inhibition field model of phyllotaxis adapted from Smith et al. (2006b), a ring of potential organ initiation (active ring) was subdivided into 360 points. The inhibition from existing primordia was calculated in each point on the active ring based on the following formula, where the total inhibition h at the ring point j is calculated as the sum of the inhibition from the n previously made primordia, with the inhibiting influence of primordia decreasing exponentially based on their age t and their distance d from the ring point.

$$h_j = \sum_{i=0}^{n} e^{-\alpha t} e^{-\beta d}$$

Here, we used $\alpha = 3$ and $\beta = 0.1$ as constants. Note that the distance between a primordium and the ring is assumed to increase linearly with time (it can be adjusted in the program parameters) and therefore is a function of both age and angle of a primordium. Due to the formula used, the minimum possible value is 0, while the maximum possible values approximate 1. As a control, we simulated plants with randomly placed leaves. However, primordia that are successively initiated at very small angles are prone to fusion in real plants and are not detectable as separate organs later in development. Therefore, we restricted the positioning of random leaves to at least 20° or more away from the previous leaf.

The source code and raw data can be found in Supplemental File S1.

Supplemental Data

The following materials are available in the online version of this article.

Supplemental Figure S1. Venation patterns in *pin1* mutants.

Supplemental Figure S2. Relationship of angles and plastochrons in rosettes.

Supplemental Figure S3. Expression of PIN-GFP in the *pin1* background.

Supplemental Figure S4. Additional phenotyping of multiple *pin* mutants.

Supplemental Figure S5. Leaf production in *pin1aux2lax1*.

Supplemental File S1. Code and input/output files for the HI calculations.

ACKNOWLEDGMENTS

We thank Alain Weber and Pierre Barbier de Reuille for helpful input on the HI and statistical testing and Saiko Yoshida and Anne-Lise Routier-Kierzkowska for critical reading of the manuscript.

Received May 15, 2012; accepted June 18, 2012; published June 21, 2012.

LITERATURE CITED

Adler I, Barabé D, Jean RV (1997) A history of the study of phyllotaxis. Ann Bot (Lond) **80:** 231–244

Bainbridge K, Guyomarc'h S, Bayer E, Swarup R, Bennett M, Mandel T, Kuhlemeier C (2008) Auxin influx carriers stabilize phyllotactic patterning. Genes Dev **22:** 810–823

Barabé D, Jeune B (2006) Complexity and information in regular and random phyllotactic patterns. Riv Biol **99:** 85–102

Barkoulas M, Hay A, Kougioumoutzi E, Tsiantis M (2008) A developmental framework for dissected leaf formation in the Arabidopsis relative Cardamine hirsuta. Nat Genet **40:** 1136–1141

Bayer EM, Smith RS, Mandel T, Nakayama N, Sauer M, Prusinkiewicz P, Kuhlemeier C (2009) Integration of transport-based models for phyllotaxis and midvein formation. Genes Dev **23:** 373–384

Benková E, Michniewicz M, Sauer M, Teichmann T, Seifertová D, Jürgens G, Friml J (2003) Local, efflux-dependent auxin gradients as a common module for plant organ formation. Cell **115:** 591–602

Besnard F, Vernoux T, Hamant O (2011) Organogenesis from stem cells in planta: multiple feedback loops integrating molecular and mechanical signals. Cell Mol Life Sci **68:** 2885–2906

Bilsborough GD, Runions A, Barkoulas M, Jenkins HW, Hasson A, Galinha C, Laufs P, Hay A, Prusinkiewicz P, Tsiantis M (2011) Model for the regulation of Arabidopsis thaliana leaf margin development. Proc Natl Acad Sci USA **108:** 3424–3429

Blilou I, Xu J, Wildwater M, Willemsen V, Paponov I, Friml J, Heidstra R, Aida M, Palme K, Scheres B (2005) The PIN auxin efflux facilitator network controls growth and patterning in Arabidopsis roots. Nature **433:** 39–44

Braybrook SA, Kuhlemeier C (2010) How a plant builds leaves. Plant Cell **22:** 1006–1018

Cheng Y, Dai X, Zhao Y (2006) Auxin biosynthesis by the YUCCA flavin monooxygenases controls the formation of floral organs and vascular tissues in Arabidopsis. Genes Dev **20:** 1790–1799

Cheng Y, Dai X, Zhao Y (2007) Auxin synthesized by the YUCCA flavin monooxygenases is essential for embryogenesis and leaf formation in *Arabidopsis*. Plant Cell **19:** 2430–2439

Ding Z, Galván-Ampudia CS, Demarsy E, Łangowski L, Kleine-Vehn J, Fan Y, Morita MT, Tasaka M, Fankhauser C, Offringa R, et al (2011) Light-mediated polarization of the PIN3 auxin transporter for the phototropic response in Arabidopsis. Nat Cell Biol **13:** 447–452

Douady S, Couder Y (1996) Phyllotaxis as a dynamical self organizing process. Part II. The spontaneous formation of a periodicity and the coexistence of spiral and whorled patterns. J Theor Biol **178:** 275–294

Dumais J (2007) Can mechanics control pattern formation in plants? Curr Opin Plant Biol **10:** 58–62

Fleming AJ, McQueen-Mason S, Mandel T, Kuhlemeier C (1997) Induction of leaf primordia by the cell wall protein expansin. Science **276:** 1415–1418

Friml J, Benková E, Blilou I, Wisniewska J, Hamann T, Ljung K, Woody S, Sandberg G, Scheres B, Jürgens G, et al (2002a) AtPIN4 mediates sink-driven auxin gradients and root patterning in Arabidopsis. Cell **108:** 661–673

Friml J, Vieten A, Sauer M, Weijers D, Schwarz H, Hamann T, Offringa R, Jürgens G (2003) Efflux-dependent auxin gradients establish the apical-basal axis of Arabidopsis. Nature **426:** 147–153

Friml J, Wiśniewska J, Benková E, Mendgen K, Palme K (2002b) Lateral relocation of auxin efflux regulator PIN3 mediates tropism in Arabidopsis. Nature **415:** 806–809

Gälweiler L, Guan C, Müller A, Wisman E, Mendgen K, Yephremov A, Palme K (1998) Regulation of polar auxin transport by AtPIN1 in Arabidopsis vascular tissue. Science **282:** 2226–2230

Geisler M, Blakeslee JJ, Bouchard R, Lee OR, Vincenzetti V, Bandyopadhyay A, Titapiwatanakun B, Peer WA, Bailly A, Richards EL, et al (2005) Cellular efflux of auxin catalyzed by the Arabidopsis MDR/PGP transporter AtPGP1. Plant J **44:** 179–194

Green PB, Steele CS, Rennich SC (1996) Phyllotactic patterns: a biophysical mechanism for their origin. Ann Bot (Lond) **77:** 515–528

Heisler MG, Ohno C, Das P, Sieber P, Reddy GV, Long JA, Meyerowitz EM (2005) Patterns of auxin transport and gene expression during primordium development revealed by live imaging of the Arabidopsis inflorescence meristem. Curr Biol **15:** 1899–1911

Hofmeister W (1868). Allgemeine Morphologie der Gewächse. *In* Handbuch der Physiologischen Botanik, Band 1, Abteilung 2. W Engelmann, Leipzig, Germany, pp 405–664

Itoh JI, Kitano H, Matsuoka M, Nagato Y (2000) Shoot organization genes regulate shoot apical meristem organization and the pattern of leaf primordium initiation in rice. Plant Cell **12:** 2161–2174

Jasinski M, Ducos E, Martinoia E, Boutry M (2003) The ATP-binding cassette transporters: structure, function, and gene family comparison between rice and Arabidopsis. Plant Physiol **131:** 1169–1177

Jönsson H, Heisler MG, Shapiro BE, Meyerowitz EM, Mjolsness E (2006) An auxin-driven polarized transport model for phyllotaxis. Proc Natl Acad Sci USA **103:** 1633–1638

Keuskamp DH, Pollmann S, Voesenek LACJ, Peeters AJM, Pierik R (2010). Auxin transport through PIN-FORMED 3 (PIN3) controls shade avoidance and fitness during competition. Proc Natl Acad Sci USA **107:** 22740–22744

Kuhlemeier C (2007) Phyllotaxis. Trends Plant Sci **12:** 143–150

Larson PR (1975) Development and organization of the primary vascular system in Populus deltoides according to phyllotaxy. Am J Bot **62:** 1084–1099

Lenhard M, Laux T (2003) Stem cell homeostasis in the Arabidopsis shoot meristem is regulated by intercellular movement of CLAVATA3 and its sequestration by CLAVATA1. Development **130:** 3163–3173

Lewis DR, Wu G, Ljung K, Spalding EP (2009) Auxin transport into cotyledons and cotyledon growth depend similarly on the ABCB19 multidrug resistance-like transporter. Plant J **60:** 91–101

Ljung K, Bhalerao RP, Sandberg G (2001) Sites and homeostatic control of auxin biosynthesis in Arabidopsis during vegetative growth. Plant J **28:** 465–474

Luschnig C, Gaxiola RA, Grisafi P, Fink GR (1998) EIR1, a root-specific protein involved in auxin transport, is required for gravitropism in Arabidopsis thaliana. Genes Dev **12:** 2175–2187

Mashiguchi K, Tanaka K, Sakai T, Sugawara S, Kawaide H, Natsume M, Hanada A, Yaeno T, Shirasu K, Yao H, et al (2011) The main auxin biosynthesis pathway in Arabidopsis. Proc Natl Acad Sci USA **108:** 18512–18517

Mattsson J, Sung ZR, Berleth T (1999) Responses of plant vascular systems to auxin transport inhibition. Development **126:** 2979–2991

Mravec J, Kubes M, Bielach A, Gaykova V, Petrásek J, Skůpa P, Chand S, Benková E, Zazímalová E, Friml J (2008) Interaction of PIN and PGP transport mechanisms in auxin distribution-dependent development. Development **135:** 3345–3354

Mravec J, Skůpa P, Bailly A, Hoyerová K, Krecek P, Bielach A, Petrásek J, Zhang J, Gaykova V, Stierhof Y-D, et al (2009) Subcellular homeostasis of phytohormone auxin is mediated by the ER-localized PIN5 transporter. Nature **459:** 1136–1140

Müller A, Guan C, Gälweiler L, Tänzler P, Huijser P, Marchant A, Parry G, Bennett M, Wisman E, Palme K (1998) AtPIN2 defines a locus of Arabidopsis for root gravitropism control. EMBO J **17:** 6903–6911

Okada K, Ueda J, Komaki MK, Bell CJ, Shimura Y (1991) Requirement of the auxin polar transport system in early stages of *Arabidopsis* floral bud formation. Plant Cell **3:** 677–684

Paponov IA, Teale WD, Trebar M, Blilou I, Palme K (2005) The PIN auxin efflux facilitators: evolutionary and functional perspectives. Trends Plant Sci **10:** 170–177

Peaucelle A, Louvet R, Johansen JN, Höfte H, Laufs P, Pelloux J, Mouille G (2008) Arabidopsis phyllotaxis is controlled by the methyl-esterification status of cell-wall pectins. Curr Biol **18:** 1943–1948

Pien S, Wyrzykowska J, McQueen-Mason S, Smart C, Fleming A (2001) Local expression of expansin induces the entire process of leaf development and modifies leaf shape. Proc Natl Acad Sci USA **98:** 11812–11817

Prasad K, Grigg SP, Barkoulas M, Yadav RK, Sanchez-Perez GF, Pinon V, Blilou I, Hofhuis H, Dhonukshe P, Galinha C, et al (2011) Arabidopsis PLETHORA transcription factors control phyllotaxis. Curr Biol **21:** 1123–1128

Prusinkiewicz P (2004) Art and science for life: designing and growing virtual plants with L-systems. Design **630:** 15–28

Rakusová H, Gallego-Bartolomé J, Vanstraelen M, Robert HS, Alabadí D, Blázquez MA, Benková E, Friml J (2011) Polarization of PIN3-dependent auxin transport for hypocotyl gravitropic response in Arabidopsis thaliana. Plant J **67:** 817–826

Reinhardt D, Frenz M, Mandel T, Kuhlemeier C (2005) Microsurgical and laser ablation analysis of leaf positioning and dorsoventral patterning in tomato. Development **132:** 15–26

Reinhardt D, Mandel T, Kuhlemeier C (2000) Auxin regulates the initiation and radial position of plant lateral organs. Plant Cell **12:** 507–518

Reinhardt D, Pesce E-R, Stieger P, Mandel T, Baltensperger K, Bennett M, Traas J, Friml J, Kuhlemeier C (2003) Regulation of phyllotaxis by polar auxin transport. Nature **426:** 255–260

Ridley JN (1982) Computer simulation of contact pressure in capitula. J Theor Biol **95:** 1–11

Scanlon MJ (2003) The polar auxin transport inhibitor N-1-naphthylphthalamic acid disrupts leaf initiation, KNOX protein regulation, and formation of leaf margins in maize. Plant Physiol **133:** 597–605

Scarpella E, Marcos D, Friml JA, Berleth T (2006) Control of leaf vascular patterning by polar auxin transport. Genes Dev **20:** 1015–1027

Schoute JC (1913) Beiträge zur Blattstellungslehre. I. Die Theorie. Rec Trav Bot Neerl **10:** 153–339

Shipman PD, Newell AC (2005) Polygonal planforms and phyllotaxis on plants. J Theor Biol **236:** 154–197

Sieburth LE (1999) Auxin is required for leaf vein pattern in Arabidopsis. Plant Physiol **121:** 1179–1190

Smith RS, Bayer EM (2009) Auxin transport-feedback models of patterning in plants. Plant Cell Environ **32:** 1258–1271

Smith RS, Guyomarc'h S, Mandel T, Reinhardt D, Kuhlemeier C, Prusinkiewicz P (2006a) A plausible model of phyllotaxis. Proc Natl Acad Sci USA **103:** 1301–1306

Smith RS, Kuhlemeier C, Prusinkiewicz P (2006b) Inhibition fields for phyllotactic pattern formation: a simulation study. Can J Bot **84:** 1635–1649

Snow M, Snow R (1931) Experiments on phyllotaxis. I. The effect of isolating a primordium. Philos Trans R Soc **221B:** 1–43

Stepanova AN, Yun J, Robles LM, Novak O, He W, Guo H, Ljung K, Alonso JM (2011) The *Arabidopsis* YUCCA1 flavin monooxygenase functions in the indole-3-pyruvic acid branch of auxin biosynthesis. Plant Cell **23:** 3961–3973

Vernoux T, Brunoud G, Farcot E, Morin V, Van den Daele H, Legrand J, Oliva M, Das P, Larrieu A, Wells D, et al (2011) The auxin signalling network translates dynamic input into robust patterning at the shoot apex. Mol Syst Biol **7:** 508–523

Verrier PJ, Bird D, Burla B, Dassa E, Forestier C, Geisler M, Klein M, Kolukisaoglu U, Lee Y, Martinoia E, et al (2008) Plant ABC proteins: a unified nomenclature and updated inventory. Trends Plant Sci **13:** 151–159

Vieten A, Vanneste S, Wisniewska J, Benková E, Benjamins R, Beeckman T, Luschnig C, Friml J (2005) Functional redundancy of PIN proteins is accompanied by auxin-dependent cross-regulation of PIN expression. Development **132:** 4521–4531

Wabnik K, Kleine-Vehn JR, Govaerts W, Friml JA (2011) Prototype cell-to-cell auxin transport mechanism by intracellular auxin compartmentalization. Trends Plant Sci **16:** 468–475

Won C, Shen X, Mashiguchi K, Zheng Z, Dai X, Cheng Y, Kasahara H, Kamiya Y, Chory J, Zhao Y (2011) Conversion of tryptophan to indole-3-acetic acid by TRYPTOPHAN AMINOTRANSFERASES OF ARABIDOPSIS and YUCCAs in Arabidopsis. Proc Natl Acad Sci USA **108:** 18518–18523

Xu J, Scheres B (2005) Dissection of *Arabidopsis* ADP-RIBOSYLATION FACTOR 1 function in epidermal cell polarity. Plant Cell **17:** 525–536

Yoshida S, Mandel T, Kuhlemeier C (2011) Stem cell activation by light guides plant organogenesis. Genes Dev **25:** 1439–1450

Žádníková P, Petrásek J, Marhavy P, Raz V, Vandenbussche F, Ding Z, Schwarzerová K, Morita MT, Tasaka M, Hejátko J, et al (2010) Role of PIN-mediated auxin efflux in apical hook development of Arabidopsis thaliana. Development **137:** 607–617

Zhao Z, Andersen SU, Ljung K, Dolezal K, Miotk A, Schultheiss SJ, Lohmann JU (2010) Hormonal control of the shoot stem-cell niche. Nature **465:** 1089–1092